

Chemodosimetric Analysis in Food-Safety Monitoring: Design, Synthesis, and Application of Bimetallic Re(I)-Pt(II) Complexes for Detection of Biogenic Sulfide Odorants in Foods

Supporting information

Cheuk-Fai Chow^{*a,b}, Fu-Wen Gong^c, Cheng-Bin Gong^{*c}

^aDepartment of Science and Environmental Studies, The Hong Kong Institute of Education, 10 Lo Ping Road, Tai Po Hong Kong SAR, China. ^bCentre for Education in Environmental Sustainability, The Hong Kong Institute of Education, 10 Lo Ping Road, Tai Po Hong Kong SAR, China. ^cCollege of Chemistry and Chemical Engineering, Southwest University, Chong Qing, China.

E-mail: cfchow@ied.edu.hk; Fax: (+852) 29487676; Tel: (+852) 29487671

EXPERIMENTAL SECTION

(i) Materials and General Procedures. The ligands (*Lig*), 2,2'-biquinoline (*biq*), 5-phenyl-1,10-phenanthroline (*5-ph-phen*), and 2,2'-bipyridine (*bpy*), $K_2(PtCl_4)$, $Re(CO)_5Cl$, KCN, dimethyl sulfide (99%), propanoic acid (99%), 4-ethylphenol (99%), and triethylamine (99%), were obtained from Aldrich. Dimethyl disulfide (99%) was obtained from Acros, and dimethyl trisulfide (98%) was purchased from TCI. Gaseous H_2S (99.5%), CO (99.95%), and CH_4 (99.9%) were obtained from Hong Kong Special Gas Company. *fac*- $[Re(Lig)(CO)_3Cl]$,¹ $Re(Lig)(CO)_3CN$,² and $Pt(DMSO)_2Cl_2$ ³ were prepared according to reported methods. All solvents used were of analytical grade.

(ii) Physical Measurements and Instrumentation. 1H NMR spectra were recorded using a Bruker AVANCE III System 400MHz NMR spectrometer. Electrospray mass spectroscopy (ESI-MS) was performed using an AB SCIEX API 2000 LC/MS/MS system. Elemental analyses were performed using a Vario EL CHN analyzer. Infrared spectra in the range 500–4000 cm^{-1} using KBr pellets were recorded on a Perkin Elmer Model Frontier FTIR spectrometer, and UV-vis spectra were measured on a Cary 50 ultraviolet-visible spectrophotometer. Emission spectra were recorded using a Horiba FluoroMax-4 spectrofluorimetric with a 5 nm slit width and 0.5 s integration time. Luminescence quantum yields were measured using the optical dilution method⁴ with an aerated aqueous solution of $[Ru(bpy)_3]Cl_2$ ($\phi = 0.028$, excitation wavelength of 455 nm)⁵ as the standard solution.

Crystal Structure Determination: Yellow-orange single-plated crystals of $[Re(biq)(CO)_3(CN)]-[Pt(DMSO)(Cl)_2]$ (**1**) were grown by slow diffusion of diethyl ether into a CH_2Cl_2 solution of the complex. Geometric and intensity data for the complexes were collected on a Bruker Smart Apex II CCD diffractometer with Cu $K\alpha$ radiation ($\lambda = 1.54180 \text{ \AA}$) at 293(2) K. The intensities were corrected for Lorentz and polarization factors, as well as for absorption using the multiscan method.⁶ All the structures of the complexes were solved by direct methods (SHELX-97)⁷ in

conjunction with standard difference Fourier techniques and subsequently refined by the full-matrix least-squares method on F^2 . Nonhydrogen atoms were refined with anisotropic displacement parameters. The hydrogen atoms were generated in their idealized positions and allowed to ride on the respective carbon atoms.

Re(*biq*)(CO)₃(CN). The complex was synthesized by modification of the method reported by Leasure^{2a} and Takeda,^{2b} as follows: An ethanol/water (2:1 v/v, 100 mL) mixture containing *fac*-[Re(*biq*)(CO)₃Cl] (0.150 g, 0.267 mmol) and KCN (1.00 g, 15.6 mmol) was refluxed under a N₂ atmosphere for 2 h. During the reaction, the red suspension clarified and became reddish black. The reaction was monitored by TLC analysis until no starting materials remained (silica gel and ethyl acetate, R_f = 0.55). The ethanol extract was evaporated and the orange crude solid suspended in water was collected by suction filtration. The complex was isolated by column chromatography on silica gel with ethyl acetate/MeOH (v/v 3:1). Two bands appeared in the column: The first band contained the organic ligand (R_f = 0.95 with purple luminescence) and the second band contained the pure product (R_f = 0.4 with red-orange luminescence). The complex was obtained as an orange solid (yield = 50%) and was characterized by ¹H-NMR, ESI-MS, IR spectroscopy, and microanalysis. (400 MHz, DMSO) δ ppm = 8.93 (d, J = 8.8 Hz, 2H), 8.89 (d, J = 9.2 Hz, 2H), 8.63 (d, J = 9.2 Hz, 2H), 8.15(d, J = 8.0 Hz, 2H), 8.04 (t, J = 5.6 Hz, 2H), 7.79 (t, J = 7.6 Hz, 2H). IR (KBr): $\nu_{\text{C}\equiv\text{N}}$ = 2122 cm⁻¹; $\nu_{\text{C}=\text{O}}$ = 2010 and 1893 cm⁻¹. ESI-MS (+ve mode): m/z 575.7 {[Re(*biq*)(CO)₃(CN)]•Na}⁺. Anal. Calcd. for C₂₂H₁₂N₃O₃Re: C, 47.82; H, 2.19; N, 7.60. Found: C, 47.21; H, 2.12; N, 7.55.

Re(5-*ph-phen*)(CO)₃(CN). An ethanol/water mixture (2:1 v/v, 100 mL) containing *fac*-[Re(5-*ph-phen*)(CO)₃Cl] (0.281 g, 0.5 mmol) and KCN (0.65 g, 10 mmol) was refluxed under a N₂ atmosphere for 24 h. During the reaction, the yellow suspension clarified and became orange. TLC analysis revealed a new spot with R_f = 0.8 and no evidence of the starting materials (silica gel and

ethyl acetate). The solution was reduced to dryness *in vacuo* and the resultant yellow crude product was extracted several times with water and diethyl ether. The yellow solid was allowed to air-dry (yield = 99%). (400 MHz, CDCl₃) δ ppm = 9.39 (s, 2H), 8.53 (m, J = 5.6 Hz, 2H), 7.96 (s, 1H), 7.87 (m, J = 5.2 Hz, 1H), 7.79 (m, 1H), 7.59 (m, 3H), 7.52 (t, J = 5.6 Hz, 2H). IR (KBr): $\nu_{\text{C}\equiv\text{N}}$ = 2119 cm⁻¹; $\nu_{\text{C}=\text{O}}$ = 2017 and 1886 cm⁻¹. ESI-MS (+ve mode): m/z 576.1 {[Re(*5-ph-phen*)(CO)₃(CN)]•Na}⁺. Anal. Calcd. for C₂₂H₁₂N₃O₃Re: C, 47.82; H, 2.19; N, 7.60. Found: C, 47.99; H, 2.21; N, 7.65.

Re(*bpy*)(CO)₃(CN). The synthesis of Re(*bpy*)(CO)₃(CN) was the same as that of Re(*5-ph-phen*)(CO)₃(CN) except that *fac*-[Re(*bpy*)(CO)₃Cl] (0.231 g, 0.5 mmol) was used instead of *fac*-[Re(*5-ph-phen*)(CO)₃Cl]. During the reaction, the yellow suspension clarified and became pale yellow. The complex was isolated as an air-stable yellow solid (yield = 98 %). (400 MHz, CDCl₃) δ ppm = 9.09 (d, J = 4.8 Hz, 2H), 8.23 (d, J = 8.4 Hz, 2H), 8.09 (m, J = 6.4 Hz, 2H), 7.56 (m, J = 6.0 Hz, 2H). IR (KBr): $\nu_{\text{C}\equiv\text{N}}$ = 2115 cm⁻¹; $\nu_{\text{C}=\text{O}}$ = 2021 and 1894 cm⁻¹. ESI-MS (+ve mode): m/z 453.9 {[Re(*bpy*)(CO)₃(CN)]•H}⁺. Anal. Calcd. for C₁₄H₈N₃O₃Re: C, 37.17; H, 1.78; N, 9.29. Found: C, 37.33; H, 1.84; N, 9.31.

[Re(*5-ph-phen*)(CO)₃(CN)]-[Pt(DMSO)(Cl)₂] (2). The synthesis of [Re(*5-ph-phen*)(CO)₃(CN)]-[Pt(DMSO)(Cl)₂] was the same as that of complex **1** except that Re(*5-ph-phen*)(CO)₃(CN)¹¹ (0.110 g, 0.2 mmol) was used instead of Re(*biq*)(CO)₃(CN). Complex **2** was formed in a methanol/chloroform mixture (1:1, 80 mL). The complex was isolated as an air-stable yellow solid in good yield (98%). (400 MHz, CDCl₃) δ ppm = 9.32 (t, J = 4.8 Hz, 2H), 8.58 (m, J = 8.4 Hz, 2H), 7.93 (m, J = 8.0 Hz, 2H), 7.83 (m, J = 5.2 Hz, 1H), 7.53 (m, J = 5.6 Hz, 5H), 3.28 (s, 6H). IR (KBr): $\nu_{\text{C}\equiv\text{N}}$ = 2169 cm⁻¹; $\nu_{\text{C}=\text{O}}$ = 2029 and 1899 cm⁻¹. ESI-MS (+ve mode): m/z 919.5 {[Re(*5-ph-phen*)(CO)₃(CN)]-[Pt(DMSO)Cl₂]•Na}⁺. TLC: silica gel and ethyl acetate/hexane (3:1), R_f = 0.55. Anal. Calcd. for C₂₄H₁₈Cl₂N₃O₄PtReS: C, 32.14; H, 2.02; N, 4.69. Found: C, 32.44; H, 2.04; N,

4.76.

[Re(*bpy*)(CO)₃(CN)]–[Pt(DMSO)(Cl)₂] (3). The synthesis of [Re(*bpy*)(CO)₃(CN)]–[Pt(DMSO)(Cl)₂] was the same as that of complex **1** except that Re(*bpy*)(CO)₃(CN)¹¹ (0.0905 g, 0.2 mmol) was used instead of Re(*biq*)(CO)₃(CN). Complex **3** was formed in a methanol/chloroform mixture (1:1, 70 mL). The complex was isolated as an air-stable yellow solid in good yield (98%). (400 MHz, CDCl₃) δ ppm = 8.99 (d, J = 4.8 Hz, 2H), 8.20–8.29 (m, 2H), 8.10–8.18 (m, 2H), 7.52–7.63 (m, 2H), 3.35 (s, 6H). IR (KBr): $\nu_{\text{C}\equiv\text{N}}$ = 2180 cm⁻¹; $\nu_{\text{C}=\text{O}}$ = 2022 and 1907 cm⁻¹. ESI-MS (+ve mode): m/z 819.5 {[Re(*bpy*)(CO)₃(CN)]–[Pt(DMSO)Cl₂]•Na}⁺. TLC: silica gel and ethyl acetate/hexane (3:1), R_f = 0.55. Anal. Calcd. for C₁₆H₁₄Cl₂N₃O₄PtReS: C, 24.13; H, 1.77; N, 5.28. Found: C, 24.08; H, 1.75; N, 5.21.

X-Ray Crystal Structure of Complex 1. A perspective of complex **1** with atom labeling is depicted in Figure 1. The two metal centers in the complex adopt a linear configuration with one Pt(DMSO)Cl₂ moiety bridged to the Re(I) centre via cyano linkages. The coordination geometry of the Pt(II) center is square planar with a *cis* orientation of the two chloro ligands and DMSO coordinated to the cyano nitrogen atom. The bond distances between the Pt(II) center and cyano nitrogen atom and between the cyano carbon and nitrogen atoms are 2.04(2) and 1.09(3) Å, respectively, and are consistent with the normal bond lengths for metal–C≡N–Pt complexes [the reported bond distances between Pt and cyano nitrogen are 1.98(15) to 2.00(10) Å and those between cyano carbons and nitrogens are 1.15(15) to 1.20(11) Å].⁸ The Re–C≡N–Pt bridges deviate slightly from linearity with bond angles of 174.4(18)° at Re–C≡N and 177.7(17)° at C≡N–Pt. The crystal data and other X-ray crystallographic experimental details are summarized in Table S2. Selected bond distances and angles are summarized in Table S3.

UV-Vis Spectroscopic and Spectrofluorimetric Titrations. All solvents used for UV-vis

absorbance and spectrofluorimetric titrations were of analytical grade. The titrations were performed in chloroform, and the measurements were recorded after equilibrium was established between the receptor and substrate. The receptor-substrate interaction was determined to be 1:1 according to the Benesi-Hildebrand equations⁹ for UV-vis absorption titration (Eq. 1), as follows:

$$\frac{A_0}{A - A_0} = \left(\frac{\epsilon_0}{\epsilon_0 - \epsilon} \right) \left(\frac{1}{K_{\text{overall}}[\text{substrate}] + 1} \right) \quad \text{-----} \quad (1)$$

where A_0 and A are the absorbance of the chromogenic reagent in the absence and presence of the substrate, respectively, and ϵ_0 and ϵ are the corresponding molar absorption coefficients of the chromogenic reagent in the absence and presence of the substrate, respectively. The formation constants (K_{overall}) were estimated from the ratio between the y-intercept and slope of the straight lines obtained by plotting $A_0/(A - A_0)$ vs. $[\text{substrate}]^{-1}$ assuming a 1:1 host-guest interaction. The energies of formation ($\Delta G^\circ/\text{kJ mol}^{-1}$) of the donor-acceptor ensembles and acceptor metal-analyte adducts were evaluated from the corresponding formation constants, as stated in Eq. 2,⁹ in which R is the gas constant and T is the temperature at which the experiments were conducted.

$$\Delta G^\circ = -RT \ln(K_{\text{overall}}) \quad \text{-----} \quad (2)$$

The detection limits were estimated from the ratio in Eq. 3 using the statistic from Student's t distribution table and the standard deviation of the relative luminescence intensity (s.d.):

$$\text{Detection Limit} = (t)(\text{s.d.}) \quad \text{-----} \quad (3)$$

Formation Constants of $[\text{Re}(\text{Lig})(\text{CO})_3(\text{CN})]$ - $[\text{Pt}(\text{DMSO})(\text{Cl})_2]$ Adducts. UV-Vis absorbance and spectrofluorimetric titrations of solutions of $[\text{Re}(\text{Lig})(\text{CO})_3(\text{CN})]$ ($\text{Lig} = \text{biq}$, 5-ph-phen and bpy , 1×10^{-4} M) by $\text{Pt}(\text{DMSO})_2(\text{Cl})_2$ (0 to 3×10^{-4} M) were performed in a methanol/chloroform

mixture (1:1). The formation constants of the $[\text{Re}(\text{Lig})(\text{CO})_3(\text{CN})]-[\text{Pt}(\text{DMSO})(\text{Cl})_2]$ adducts were determined by fitting the titration curves with the 1:1 Benesi-Hildebrand equation (Eq. 1).

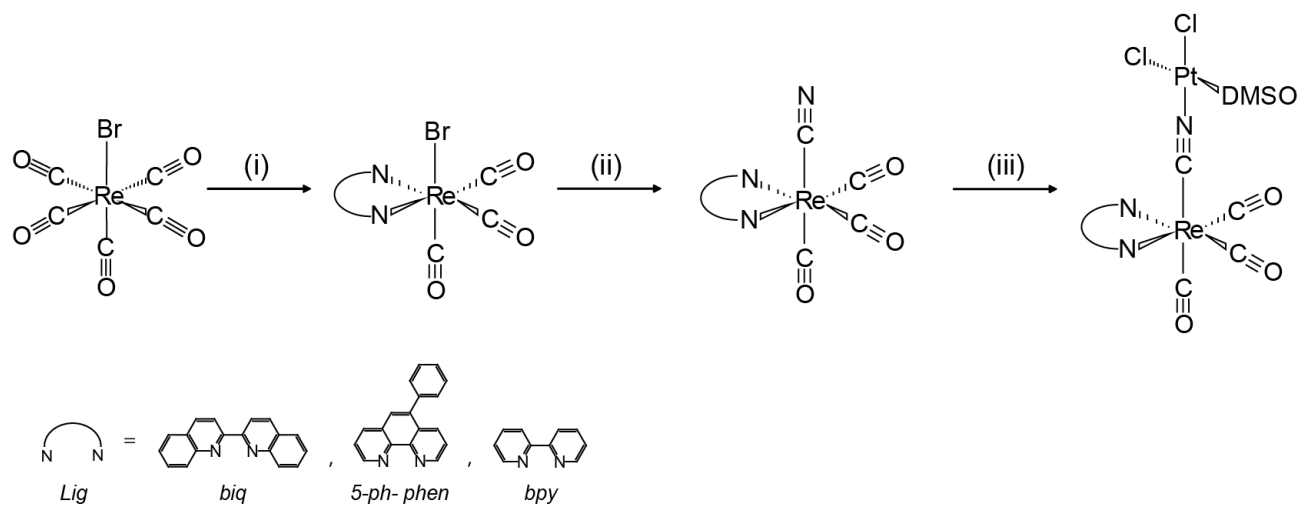
Formation Constants of $[\text{Pt}(\text{analyte})(\text{DMSO})\text{Cl}_2]$ Adducts. UV-Vis absorbance spectroscopic titrations of solutions of $\text{Pt}(\text{DMSO})_2(\text{Cl})_2$ (1×10^{-4} M) and $\text{Pt}(\text{DMSO})_2(\text{Cl})_2$ (3×10^{-4} M) by sulfide-containing analytes (dimethyl sulfide, dimethyl disulfide, dimethyl trisulfide, and H_2S) (0 to 5×10^{-4} M) and other BVC analytes (propanoic acid, 4-ethylphenol, triethylamine, CO, CH_4 , and N_2) (0 to 2×10^{-1} M), respectively, were carried out in a methanol/chloroform mixture (1:1). The formation constants of the $[\text{Pt}(\text{analyte})(\text{DMSO})\text{Cl}_2]$ adducts were analyzed by fitting the titration curves with the 1:1 Benesi-Hildebrand equation (Eq. 1). Gibbs free energy changes (ΔG°) were analyzed by fitting K_{overall} with Eq. 2.

Selectivity of Complexes 1–3 toward Various Analytes. A series of BVCs (dimethyl sulfide, dimethyl disulfide, dimethyl trisulfide, propanoic acid, 4-ethylphenol, triethylamine, H_2S , CO, CH_4 , and N_2) (0 to 5×10^{-4} M) were mixed with solutions of complexes **1–3** (1×10^{-4} M). The titrations were performed in chloroform at room temperature. The UV-Vis absorbance and spectrofluorimetric changes of the resulting mixtures were plotted as a function of the mole fraction of the analyte. The luminescent responses of complex **1** to the analytes were also recorded by digital photography.

Detection Limits of Complex 1 toward Dimethyl Sulfide. A series of ten chloroform solutions of **1** (1×10^{-4} M) were mixed with a fixed known concentration of dimethyl sulfide. The changes in the emissions of the resultant mixtures were recorded. The detection limits were calculated using Eq. 3.

Reference

1. Pfennig, B. W.; Chen, P.; Meyer, T. J. *Inorg. Chem.* **1996**, *35*, 2898.
2. (a) Leasure, R. M.; Sacksteder, L.; Nesselrodt, D.; Reitz, G. A.; Demas, J. N.; DeGraff, B. A. *Inorg. Chem.* **1991**, *30*, 3722–3728; (b) Takeda, H.; Koike, K.; Inoue, H.; Ishitani, O. *J. Am. Chem. Soc.* **2008**, *130*, 2023–2031.
3. Prices, J. H.; Williamson, A. N.; Schramln R. F.; Wayland, B. B. *Inorg. Chem.*, **1972**, *11*, 1280.
4. CrystalClear, Version 1.3.5; Rigaku Corp., Woodlands, TX, 1999.
5. Demas, J. N.; Crosby, G. A. *J. Phys. Chem.*, **1971**, *75*, 991.
6. Nakamaru, K. *Bull. Chem. Soc. Jpn.*, **1982**, *55*, 2697.
7. Sheldrick, G. M. SHELXTL, Crystallographic Software Package, Version 5.1; Bruker-AXS, Madison, WI, 1998.
8. (a) Chae, M. Y.; Czarnik, A. W. *J. Am. Chem. Soc.*, **1992**, *114*, 9704; (b) Czarnik, A. W.; Dujols V.; Ford, F. *J. Am. Chem. Soc.*, **1997**, *119*, 7386.
9. Connors, K. A. *Binding Constants, The Measurement of Molecular Complexes Stability*; John Wiley and Sons: New York, 1987.



Scheme S1. Synthesis of $[\text{Re}(\text{Lig})(\text{CO})_3(\text{CN})]-[\text{Pt}(\text{DMSO})(\text{Cl})_2]$ (**1-3**). Reaction conditions: (i) Reflux with appropriate ligand (*biq*, *5-ph-phen* or *bpy*) in toluene; (ii) reflux with one equivalent of NaCN in aqueous acetone; (iii) stir with one equivalent of $[\text{Pt}(\text{DMSO})_2\text{Cl}_2]$ in a methanol/chloroform mixture (1:1) in open atmosphere at room temperature.

Table S1. IR spectroscopic properties of *fac*-[Re(Lig)(CO)₃(CN)] and [Re(Lig)(CO)₃(CN)]-[Pt(DMSO)(Cl)₂] [Lig: *biq* (1), *5-ph-phen* (2) and *bpy* (3)] complexes.

Complex	IR	
	$\nu_{C\equiv N}/\text{cm}^{-1}$	$\nu_{C\equiv O} \text{ cm}^{-1}$
Re(<i>biq</i>)(CO)₃(CN)	2122 (w)	2010 (s), 1893 (s)
Re(<i>5-ph-phen</i>)(CO)₃(CN)	2119 (w)	2017 (s), 1886 (s)
Re(<i>bpy</i>)(CO)₃(CN)	2115 (w)	2021 (s), 1894 (s)
(1)	2169 (w)	2022 (s), 1903 (s)
(2)	2169 (w)	2029 (s), 1899 (s)
(3)	2180 (w)	2022 (s), 1907 (s)

^aThe infrared spectra were obtained with KBr pellets; “w” represents a weak transmission while “s” represents a strong transmission.

Table S2. Crystallographic data for [Re(*biq*)(CO)₃(CN)]–[Pt(DMSO)(Cl)₂] (1).

Empirical formula	C ₂₄ H ₁₈ Cl ₂ N ₃ O ₄ PtReS
Formula weight	896.66
Temperature, K	276(2)
Wavelength, Å	0.71073
Crystal system	Triclinic
Space group	<i>P</i> $\bar{1}$
<i>a</i> , Å	8.9082(12)
<i>b</i> , Å	10.0279(14)
<i>c</i> , Å	15.453(2)
α , deg	79.764(3)
β , deg	85.457(3)
γ , deg	88.478(3)
Volume, Å ³	1354.1(3)
<i>Z</i>	2
Density (calculated), mg m ⁻³	2.199
Absorption coefficient, mm ⁻¹	9.935
<i>F</i> (000)	836
Crystal dimensions, mm	0.30 × 0.20 × 0.10
θ range for data collection, deg	1.34 to 25.25
Limiting indices	<i>h</i> : –8 to 10; <i>k</i> : –12 to 12; <i>l</i> : –18 to 18
Reflections collected	21363
Unique reflections	4888
<i>R</i> _{int}	0.1781
Completeness to $\theta = 25.25^\circ$, %	99.6
Max. and min. transmission	0.7419 and 0.4619
Data/restraints/parameters	4888/0/325
Goodness-of-fit on <i>F</i> ²	0.999
Final <i>R</i> indices [<i>I</i> > 2 σ (<i>I</i>)]	<i>R</i> ₁ = 0.0727, <i>wR</i> ₂ = 0.1621
<i>R</i> indices (all data)	<i>R</i> ₁ = 0.1207, <i>wR</i> ₂ = 0.1894
Largest different peak and hole, eÅ ⁻³	1.498, –1.752

Table S3. Selected bond lengths (Å) and angles (°) of [Re(*biq*)(CO)₃(CN)]–[Pt(DMSO)(Cl)₂] (1).

Selected Bond Lengths (Å)			
Re(1)–N(1)	2.211(13)	Pt(1)–N(3)	2.04(2)
Re(1)–N(2)	2.220(15)	Pt(1)–S(1)	2.212(5)
Re(1)–C(19)	1.91(2)	Pt(1)–Cl(1)	2.296(5)
Re(1)–C(20)	1.899(19)	Pt(1)–Cl(2)	2.325(6)
Re(1)–C(21)	1.92(3)	C(19)–O(1)	1.14(2)
Re(1)–C(22)	2.092(17)	C(20)–O(2)	1.14(2)
C(22)–N(3)	1.09(3)	C(21)–O(3)	1.13(3)

Selected Bond angles (°)			
Re(1)–C(22)–N(3)	174.4(18)	C(22)–N(3)–Pt(1)	177.7(17)
C(20)–Re(1)–C(19)	91.5(9)	Cl(1)–Pt(1)–Cl(2)	90.9(2)
C(20)–Re(1)–C(21)	86.4(9)	Cl(1)–Pt(1)–N(3)	87.2(5)
C(19)–Re(1)–C(21)	90.4(10)	N(3)–Pt(1)–S(1)	92.0(5)
C(19)–Re(1)–C(22)	178.4(9)	S(1)–Pt(1)–Cl(2)	89.9(2)

Table S4. Electronic absorption and photoluminescence data for *fac*-[Re(Lig)(CO)₃(CN)] and [Re(Lig)(CO)₃(CN)]-[Pt(DMSO)(Cl)₂] [Lig: *biq* (**1**), *5-ph-phen* (**2**), and *bpy* (**3**)] complexes at 298 K.

Complex	Medium	$\lambda_{\text{abs}}/\text{nm}$ ($\epsilon/\text{dm}^3 \text{ mol}^{-1} \text{ cm}^{-1}$)	Emission λ/nm (quantum yield ϕ)
Re(<i>biq</i>)(CO) ₃ (CN)	CHCl ₃	267 (58225), 356 (22650), 375 (33850), 431 (6450)	675 (3×10^{-4})
	MeCN	264 (58675), 354 (22575), 372 (33100), 420sh (6675)	669 (5×10^{-5})
Re(<i>5-ph-phen</i>)(CO) ₃ (CN)	CHCl ₃	281 (28100), 382sh (8725)	551 (0.093)
	MeCN	281 (32925), 370sh (8950)	567 (0.016)
Re(<i>bpy</i>)(CO) ₃ (CN)	CHCl ₃	241 (57000), 287 (22275), 371 (20525)	559 (0.052)
	MeCN	245 (23225), 315 (14175), 351 (7725)	574 (0.028)
1	CHCl ₃	267 (47875), 358 (18900), 377 (26350), 426sh (5975)	651 (8×10^{-4})
	MeCN	266 (50800), 356 (19975), 373 (27100), 423sh (5650)	652 (4×10^{-4})
2	CHCl ₃	287 (29500), 378sh (7300)	540 (0.088)
	MeCN	285 (34100), 373sh (7625)	549 (0.014)
3	CHCl ₃	287 (21125), 319 (13675), 360sh (8625)	542 (0.005)
	MeCN	243 (30375), 316 (16725), 351sh (8700)	555 (0.004)

^aEmission quantum yields of $\lambda_{\text{em}} = 400\text{--}700 \text{ nm}$, $\lambda_{\text{ex}} = 363\text{--}432 \text{ nm}$; ^b ϕ were measured using aerated CHCl₃ or acetonitrile solutions of [Ru(*bpy*)₃]Cl₂ as the standard.

Table S5. Binding constants ($\log K_{overall}$) and Gibbs free energy changes (ΔG°) for complexation of various BVCs and $\text{Re}(\text{Lig})(\text{CO})_3(\text{CN})$ with $\text{Pt}(\text{DMSO})_2\text{Cl}_2$.

	Acceptor	Donor	$\log K_{overall}^b$	ΔG° /kJmol ⁻¹
1	$\text{Pt}(\text{DMSO})_2\text{Cl}_2$	$\text{Re}(\text{bpy})(\text{CO})_3(\text{CN})$	4.01	-22.9
2	$\text{Pt}(\text{DMSO})_2\text{Cl}_2$	$\text{Re}(\text{5-ph-phen})(\text{CO})_3(\text{CN})$	3.98	-22.7
3	$\text{Pt}(\text{DMSO})_2\text{Cl}_2$	CH_3SCH_3	3.87	-22.1
4	$\text{Pt}(\text{DMSO})_2\text{Cl}_2$	$\text{Re}(\text{biq})(\text{CO})_3(\text{CN})$	3.76	-21.5
5	$\text{Pt}(\text{DMSO})_2\text{Cl}_2$	CH_3SSCH_3	3.62	-20.7
6	$\text{Pt}(\text{DMSO})_2\text{Cl}_2$	$\text{CH}_3\text{SSSCH}_3$	3.61	-20.6
7	$\text{Pt}(\text{DMSO})_2\text{Cl}_2$	Carbon monoxide ^a	1.94	-11.1
8	$\text{Pt}(\text{DMSO})_2\text{Cl}_2$	4-Ethylphenol	1.58	-9.0
9	$\text{Pt}(\text{DMSO})_2\text{Cl}_2$	Triethylamine	0.49	-2.8
10	$\text{Pt}(\text{DMSO})_2\text{Cl}_2$	Propanoic acid	0.27	-2.5
11	$\text{Pt}(\text{DMSO})_2\text{Cl}_2$	Methane	--- ^c	--- ^c
12	$\text{Pt}(\text{DMSO})_2\text{Cl}_2$	Nitrogen	--- ^c	--- ^c
13	$\text{Pt}(\text{DMSO})_2\text{Cl}_2$	Air	--- ^c	--- ^c

^aLog $K_{overall}$ and Gibbs free energy changes are cited from the SC-Database. ^bAll donor–acceptor binding strengths were measured by UV spectroscopic titration in a methanol/chloroform mixture (v/v 1:1), at 25 °C. ^cToo small to be determined.

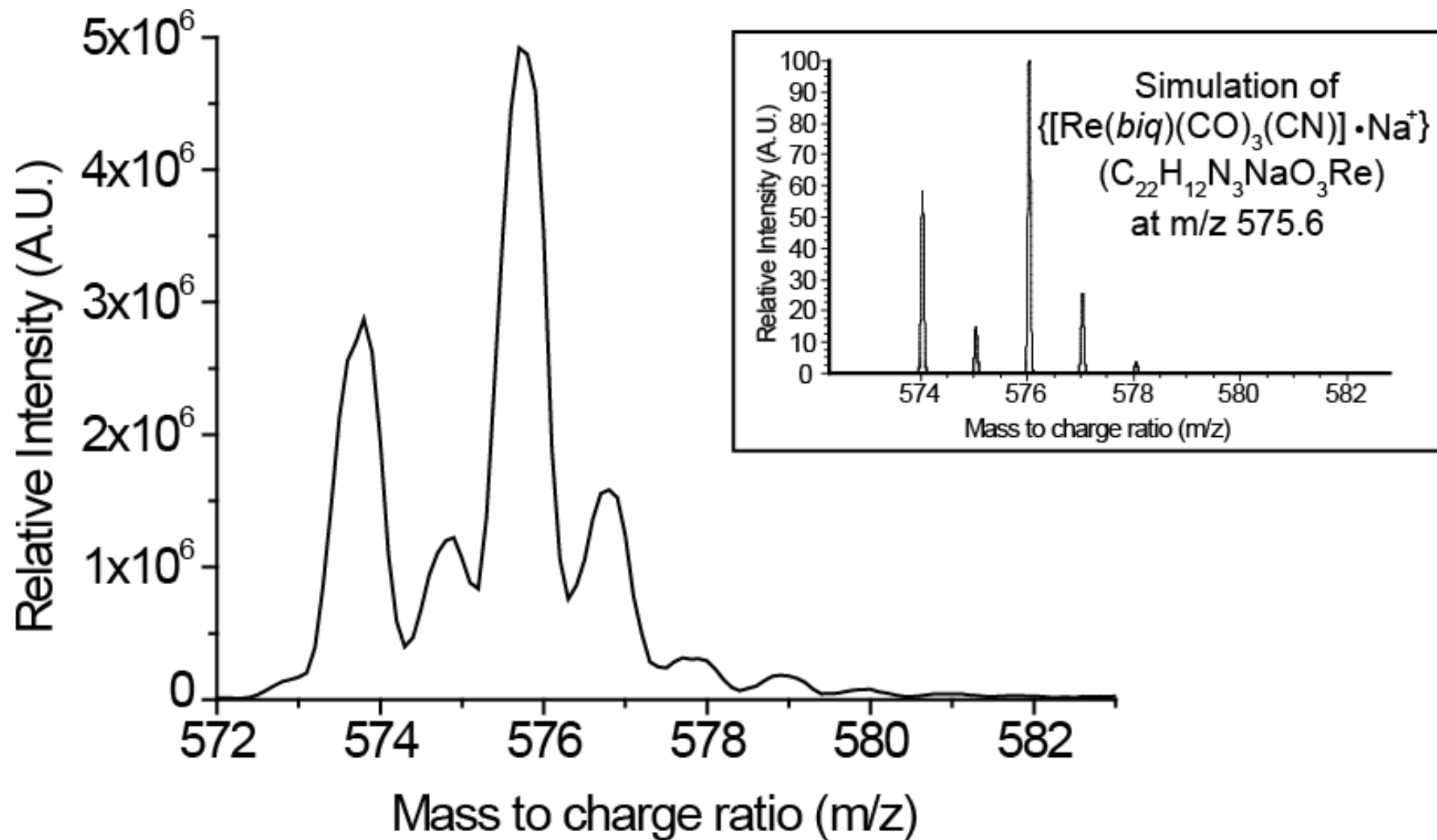


Fig S1. Electrospray mass spectra of the isotopic distribution of $\text{Re}(\text{biq})(\text{CO})_3(\text{CN})$ and (**inset**) its simulation of $\{[\text{Re}(\text{biq})(\text{CO})_3(\text{CN})] \cdot \text{Na}\}^+$ peak at 575.6. All the mass spectra were performed in methanol.

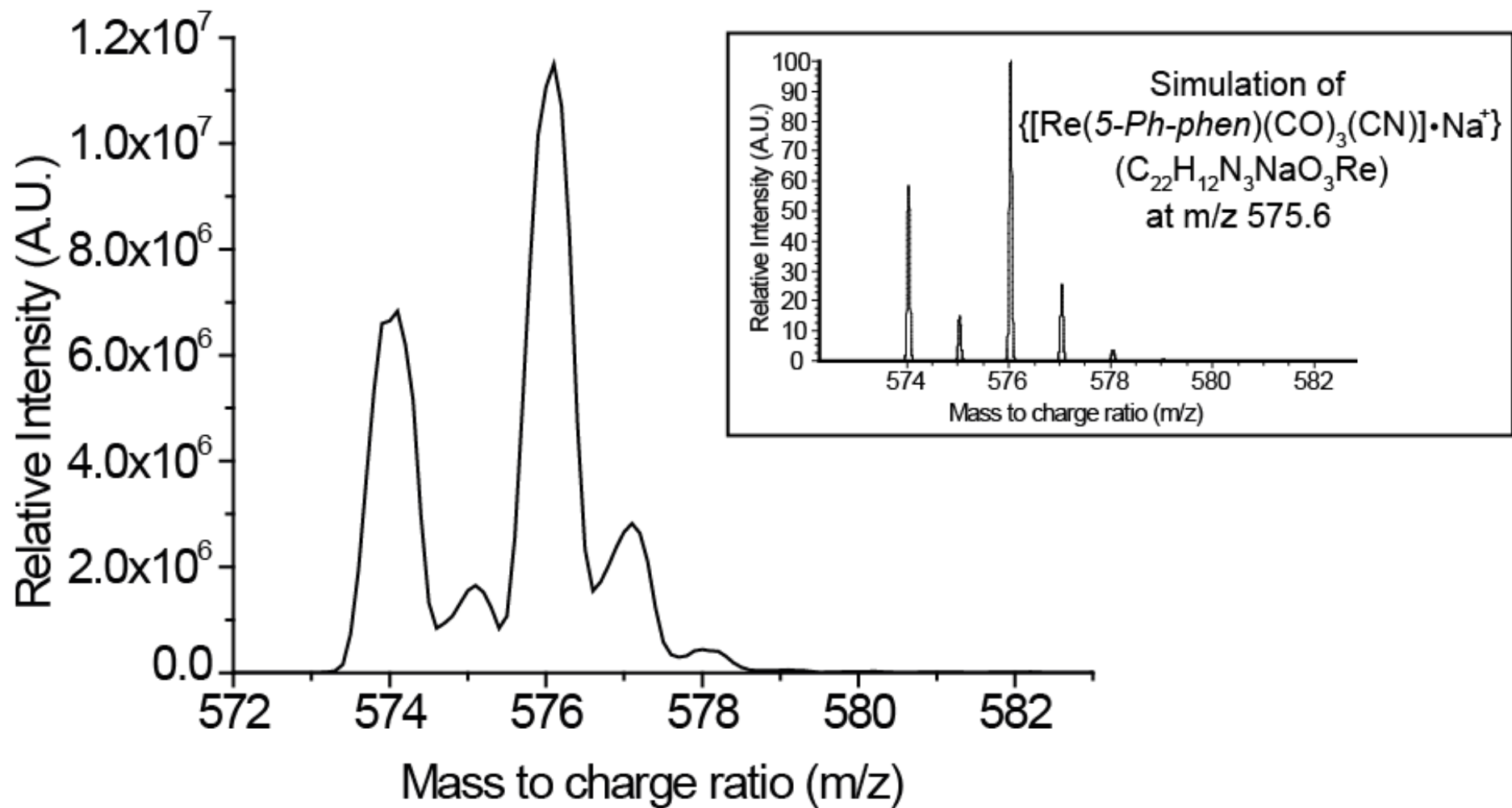


Fig S2. Electrospray mass spectra of the isotopic distribution of $\text{Re}(5\text{-}ph\text{-}phen)(\text{CO})_3(\text{CN})$ and (**inset**) its simulation of $\{[\text{Re}(5\text{-}ph\text{-}phen)(\text{CO})_3(\text{CN})] \cdot \text{Na}\}^+$ peak at 575.6. All the mass spectra were performed in methanol.

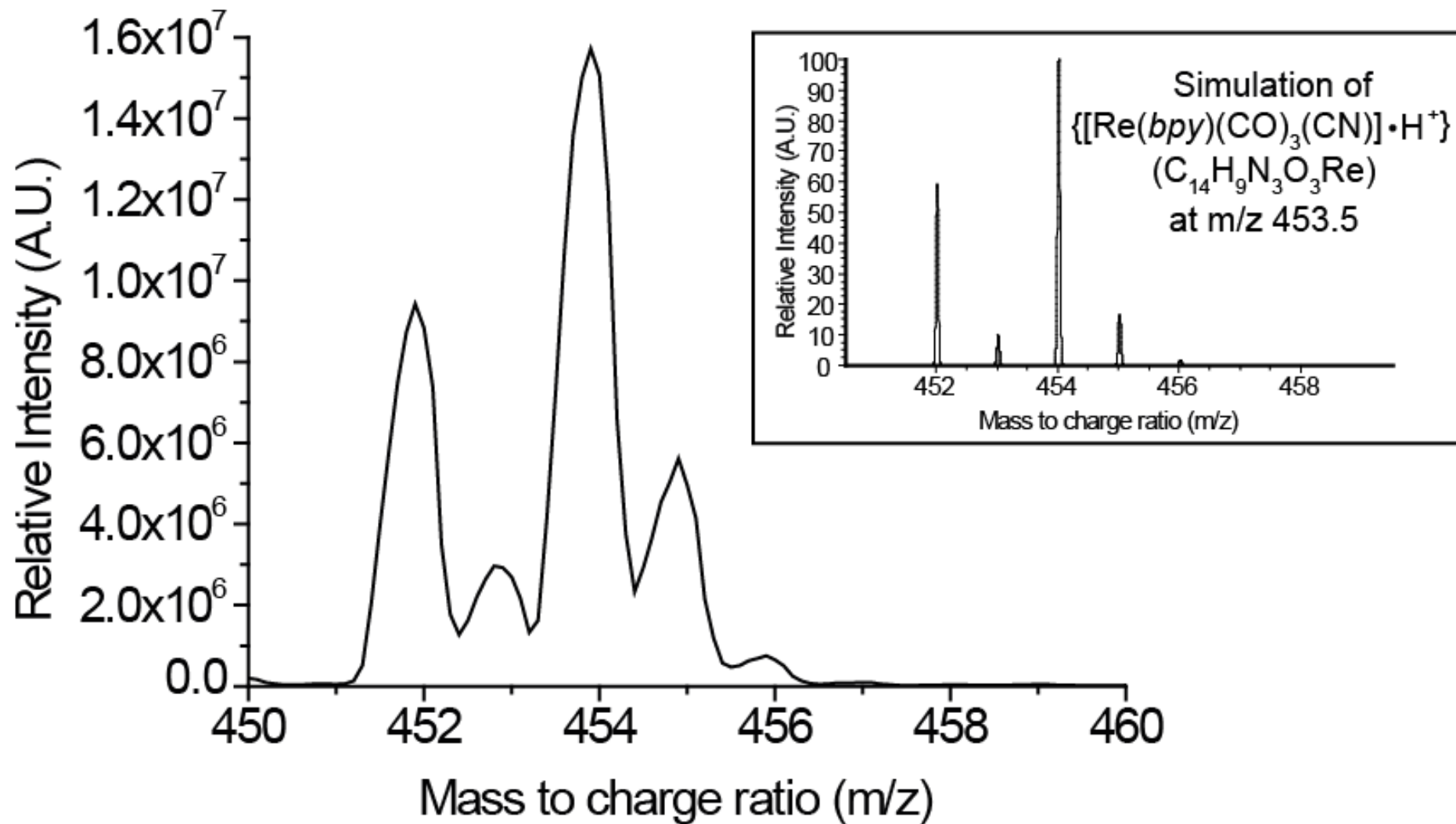


Fig S3. Electrospray mass spectra of the isotopic distribution of $\text{Re}(\text{bpy})(\text{CO})_3(\text{CN})$ and (**inset**) its simulation of $\{[\text{Re}(\text{bpy})(\text{CO})_3(\text{CN})] \cdot \text{H}^+\}$ peak at 453.5. All the mass spectra were performed in methanol.

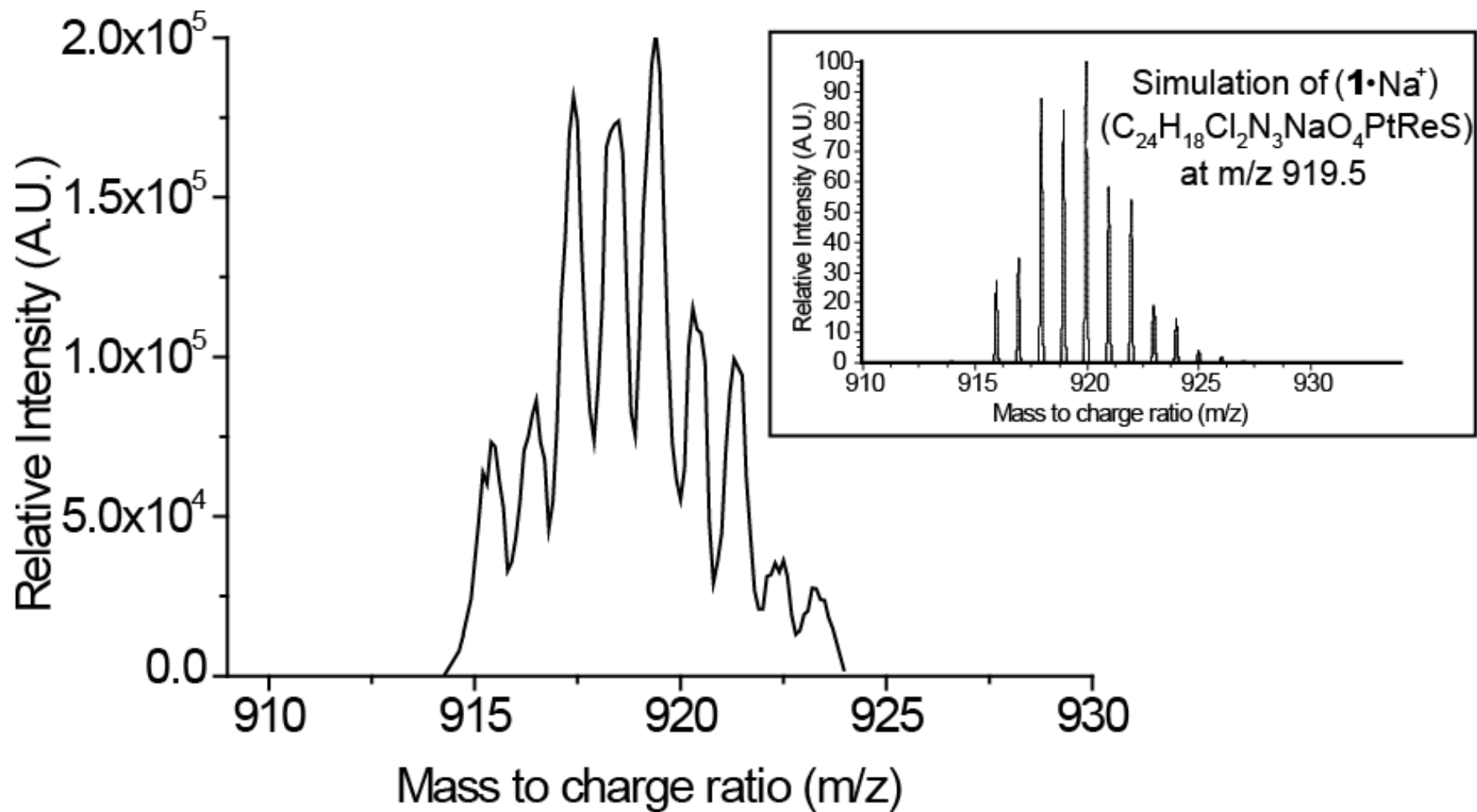


Fig S4. Electrospray mass spectra of the isotopic distribution of complex **1** and (**inset**) its simulation of $\{[\text{Re}(\text{biq})(\text{CO})_3(\text{CN})]^- [\text{Pt}(\text{DMSO})\text{Cl}_2] \cdot \text{Na}\}^+$ peak at 919.5. All the mass spectra were performed in dichloromethane/methanol mixture.

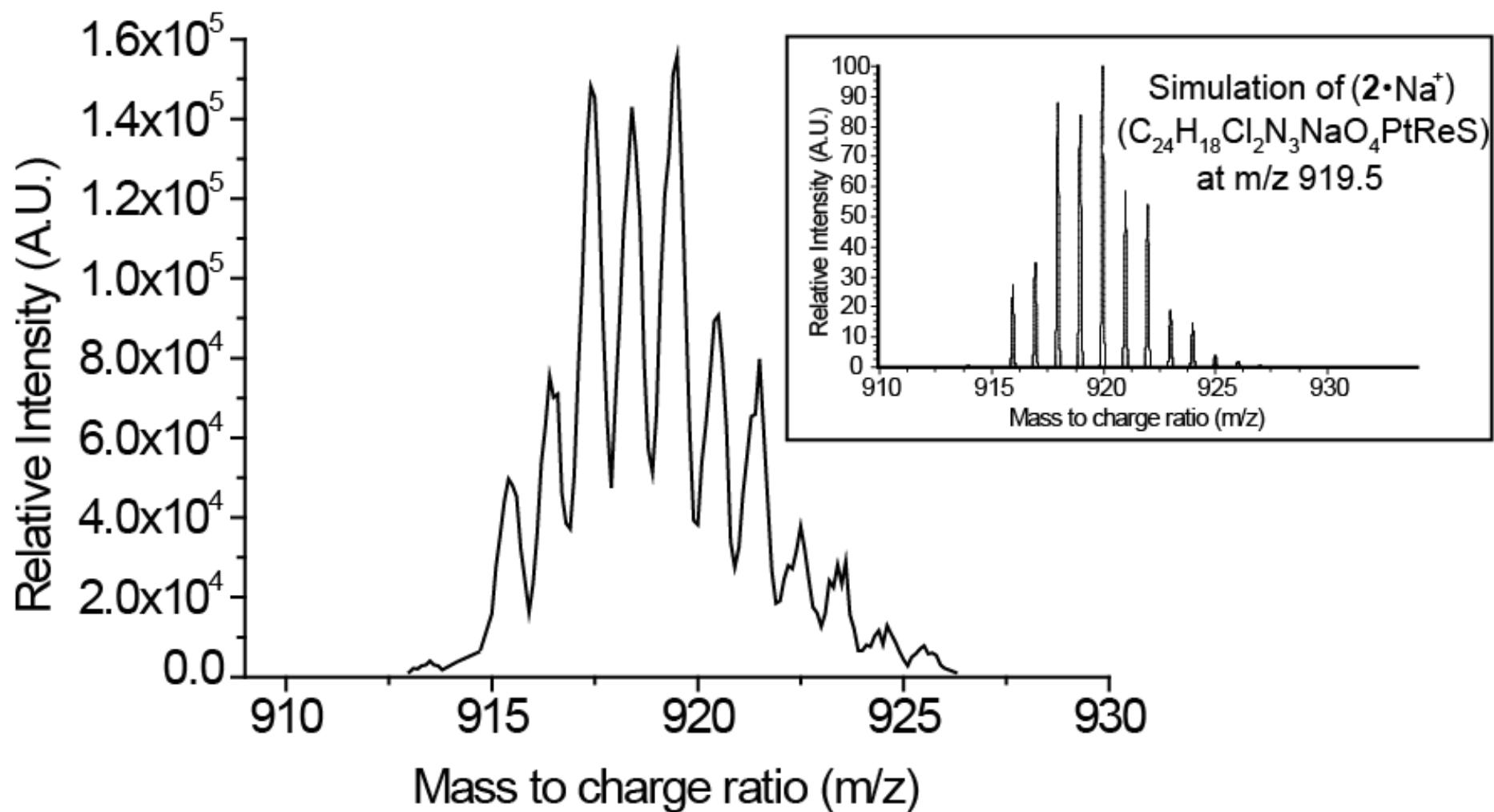


Fig S5. Electrospray mass spectra of the isotopic distribution of complex **2** and (**inset**) its simulation of $\{[\text{Re}(5\text{-}ph\text{-}phen)(\text{CO})_3(\text{CN})]^- [\text{Pt}(\text{DMSO})\text{Cl}_2] \cdot \text{Na}\}^+$ peak at 919.5. All the mass spectra were performed in dichloromethane/methanol mixture.

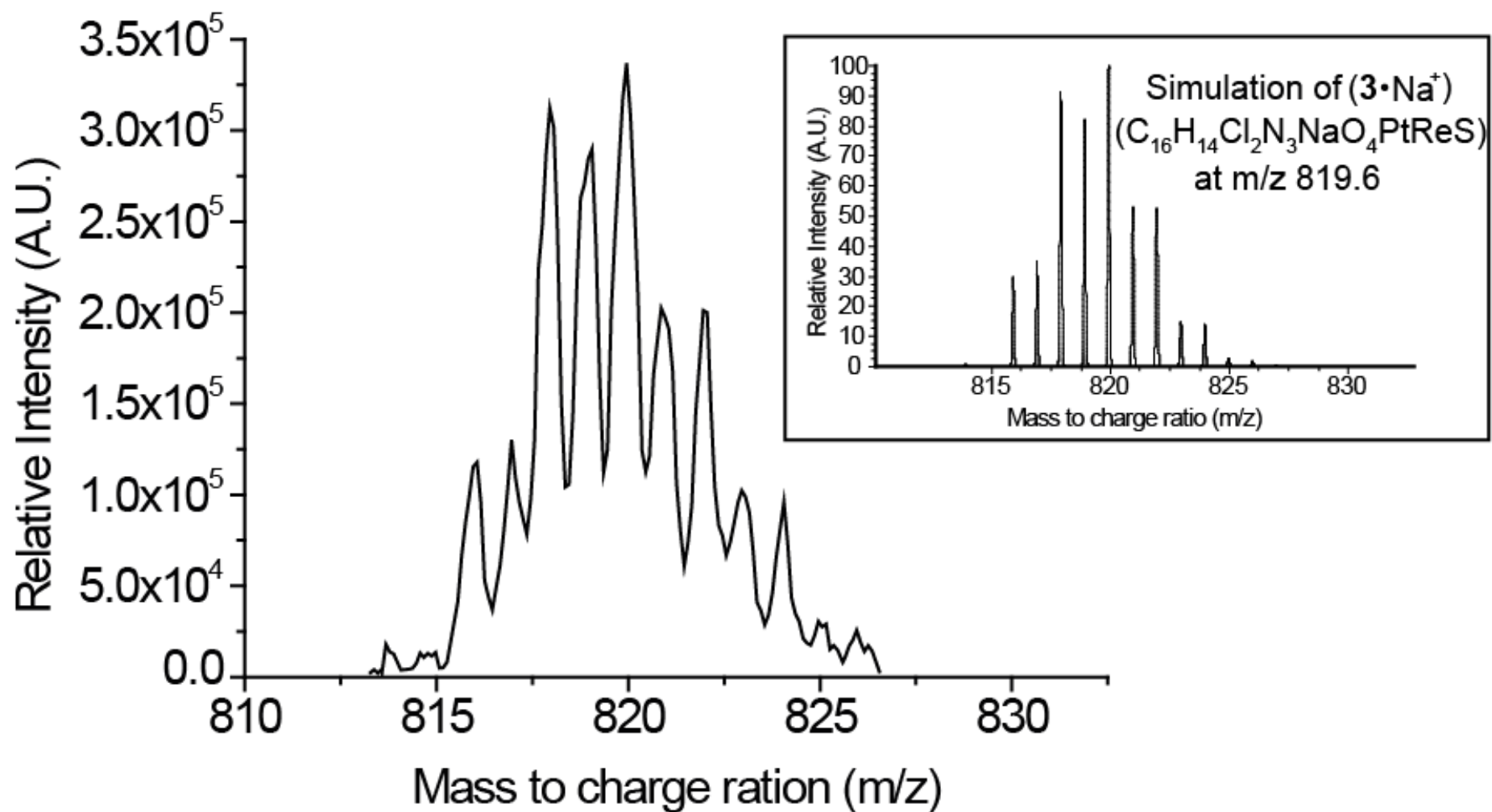
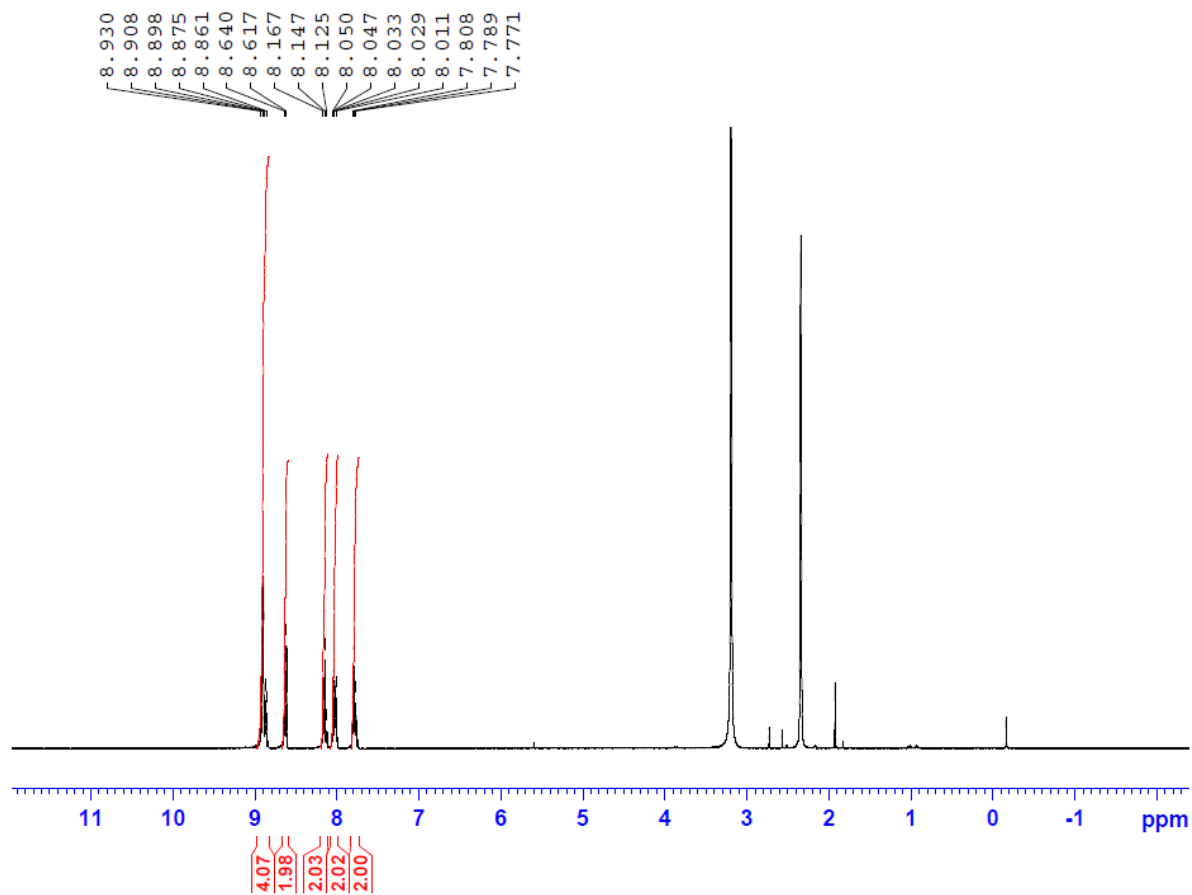


Fig S6. Electrospray mass spectra of the isotopic distribution of complex **3** and (**inset**) its simulation of $\{[\text{Re}(\text{bpy})(\text{CO})_3(\text{CN})]^- [\text{Pt}(\text{DMSO})\text{Cl}_2] \cdot \text{Na}\}^+$ peak at 819.6. All the mass spectra were performed in dichloromethane/methanol mixture.

Re-003-CN-2 20130124

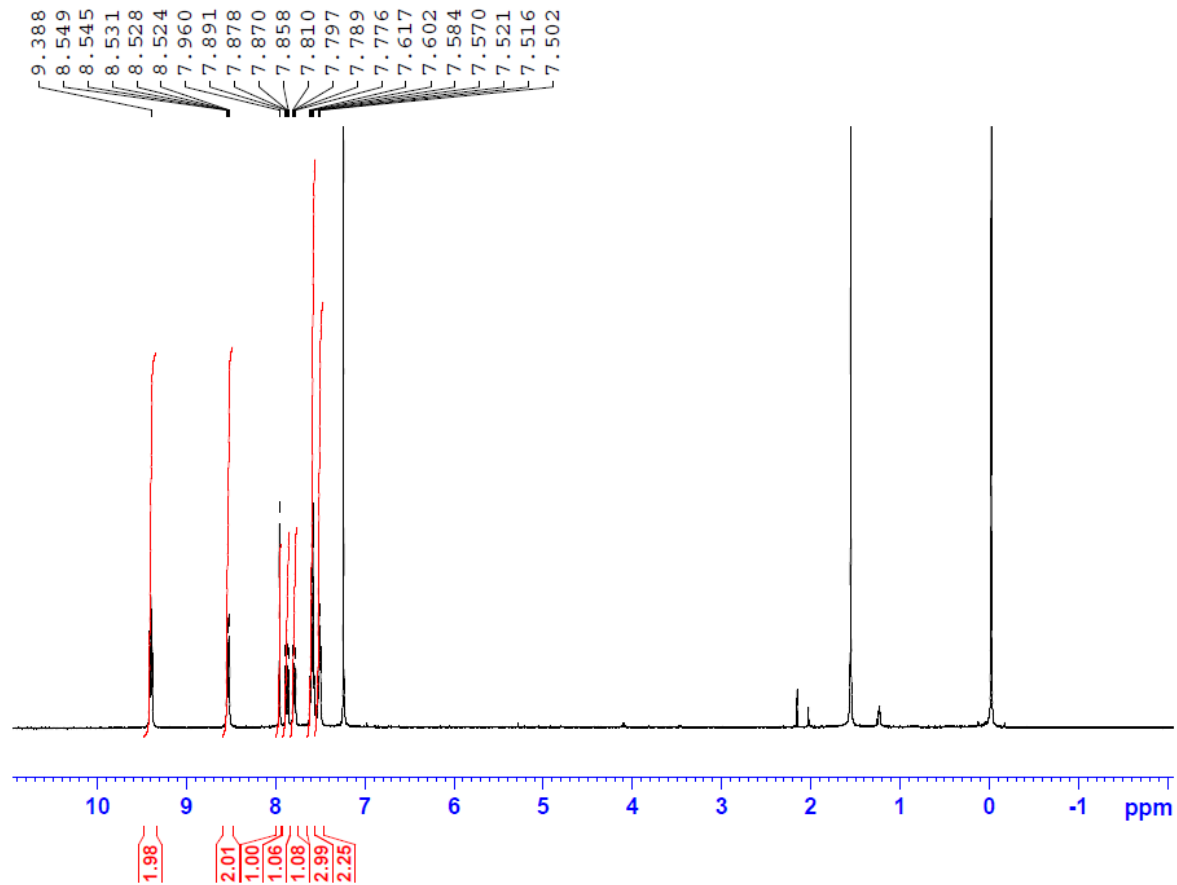


```
NAME      Fai complex
EXPNO     25
PROCNO    1
Date_     20130124
Time      19.13
INSTRUM   spect
PROBHD    5 mm PABBO BB-
PULPROG   zg30
TD         65536
SOLVENT   DMSO
NS         16
DS         2
SWH        8223.685 Hz
FIDRES     0.125483 Hz
AQ         3.9846387 sec
RG         203
DW         60.800 usec
DE         6.50 usec
TE         293.9 K
D1         1.00000000 sec
TD0        1
```

```
===== CHANNEL f1 =====
NUC1       1H
P1         14.04 usec
PL1        -2.00 dB
PL1W       17.39728355 W
SFO1       400.1424710 MHz
SI         32768
SF         400.1400588 MHz
WDW        EM
SSB        0
LB         0.30 Hz
GB         0
PC         1.00
```

Fig S7. $^1\text{H-NMR}$ spectrum of $\text{Re}(\text{biq})(\text{CO})_3(\text{CN})$ (400 MHz, d_6 -DMSO).

Re-001-CN-pt-20130125

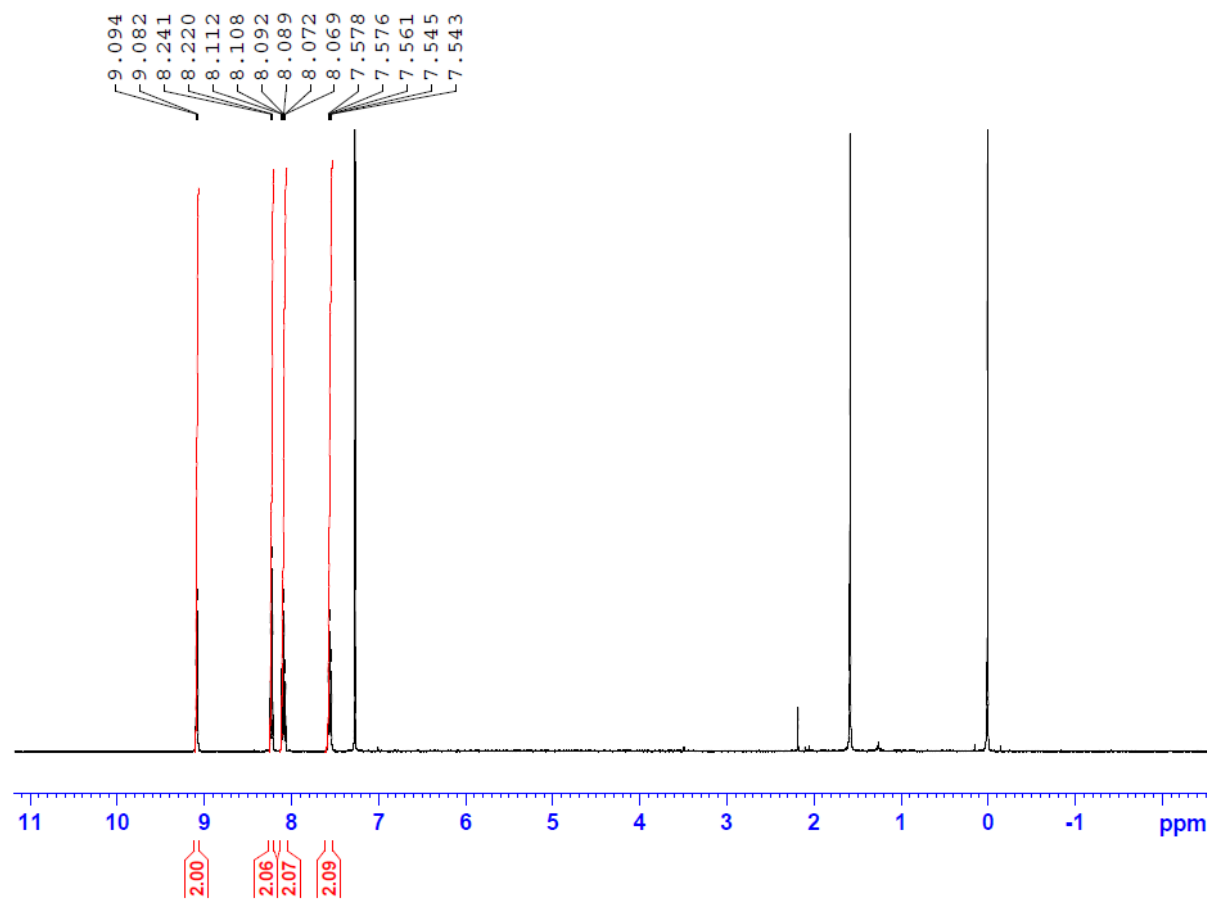


```
NAME          Fai complex
EXPNO         28
PROCNO        1
Date_         20130125
Time          19.35
INSTRUM       spect
PROBHD        5 mm PABBO BB-
PULPROG       zg30
TD            65536
SOLVENT       CDCl3
NS            16
DS            2
SWH           8223.685 Hz
FIDRES        0.125483 Hz
AQ            3.9846387 sec
RG            203
DW            60.800 usec
DE            6.50 usec
TE            293.2 K
D1            1.00000000 sec
TD0           1
```

```
===== CHANNEL f1 =====
NUC1          1H
P1            14.04 usec
PL1           -2.00 dB
PL1W         17.39728355 W
SF01         400.1424710 MHz
SI            32768
SF           400.1400122 MHz
WDW           EM
SSB           0
LB            0.30 Hz
GB            0
PC            1.00
```

Fig S8. $^1\text{H-NMR}$ spectrum of $\text{Re}(5\text{-ph-phen})(\text{CO})_3(\text{CN})$ (400 MHz, CDCl_3).

Re-004-CN-20130125

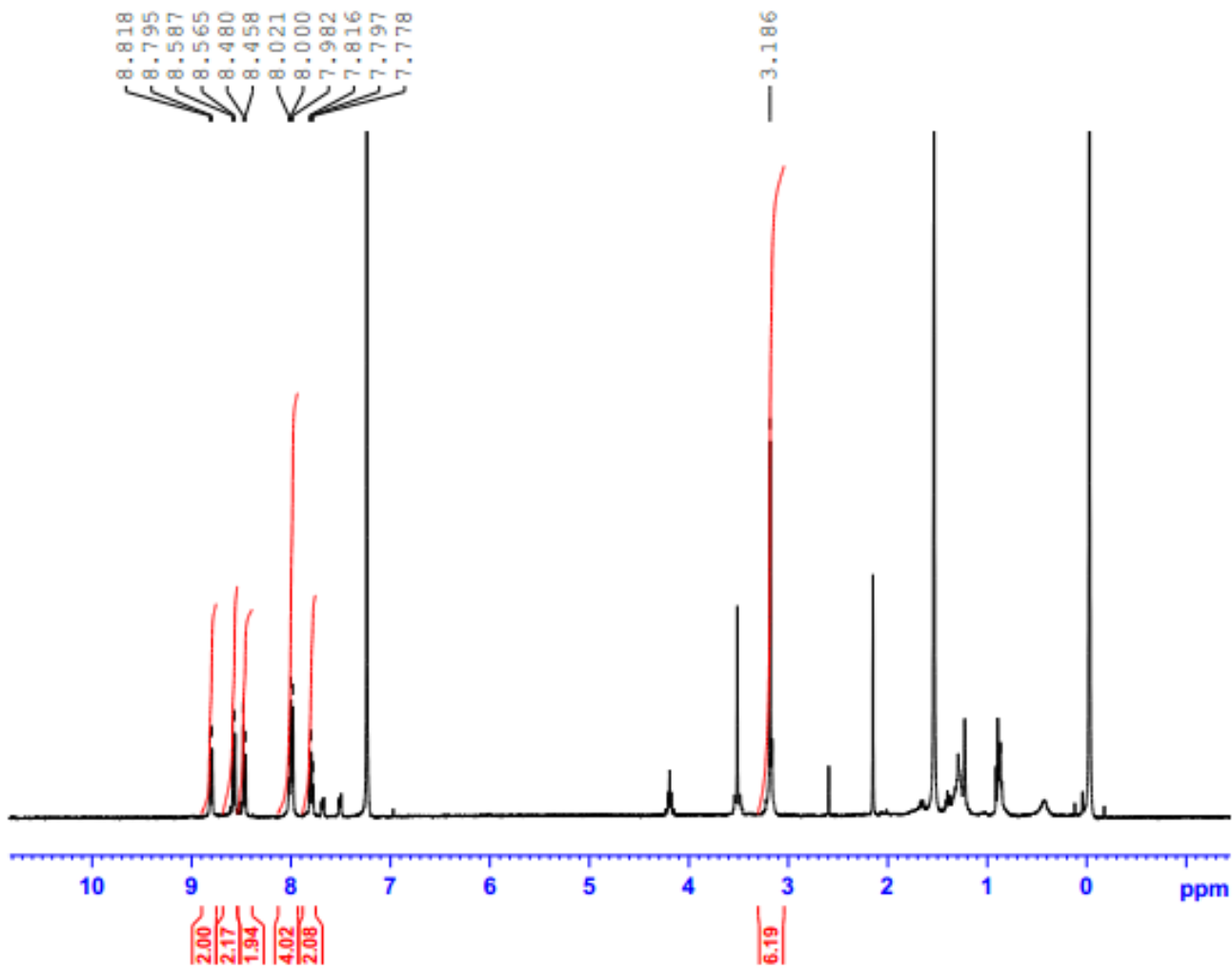


```
NAME      Fai complex
EXPNO     32
PROCNO    1
Date_     20130125
Time      20.19
INSTRUM   spect
PROBHD    5 mm PABBO BB-
PULPROG   zg30
TD         65536
SOLVENT   CDCl3
NS         16
DS         2
SWH        8223.685 Hz
FIDRES     0.125483 Hz
AQ         3.9846387 sec
RG         203
DW         60.800 usec
DE         6.50 usec
TE         293.2 K
D1         1.00000000 sec
D10        1
TDO        1
```

```
===== CHANNEL f1 =====
NUC1      1H
P1         14.04 usec
PL1        -2.00 dB
PL1W      17.39728355 W
SF01      400.1424710 MHz
SI         32768
SF         400.1400000 MHz
WDW        EM
SSB         0
LB         0.30 Hz
GB         0
PC         1.00
```

Fig S9. $^1\text{H-NMR}$ spectrum of $\text{Re}(\text{bpy})(\text{CO})_3(\text{CN})$ (400 MHz, CDCl_3).

Re-003-CN-Pt

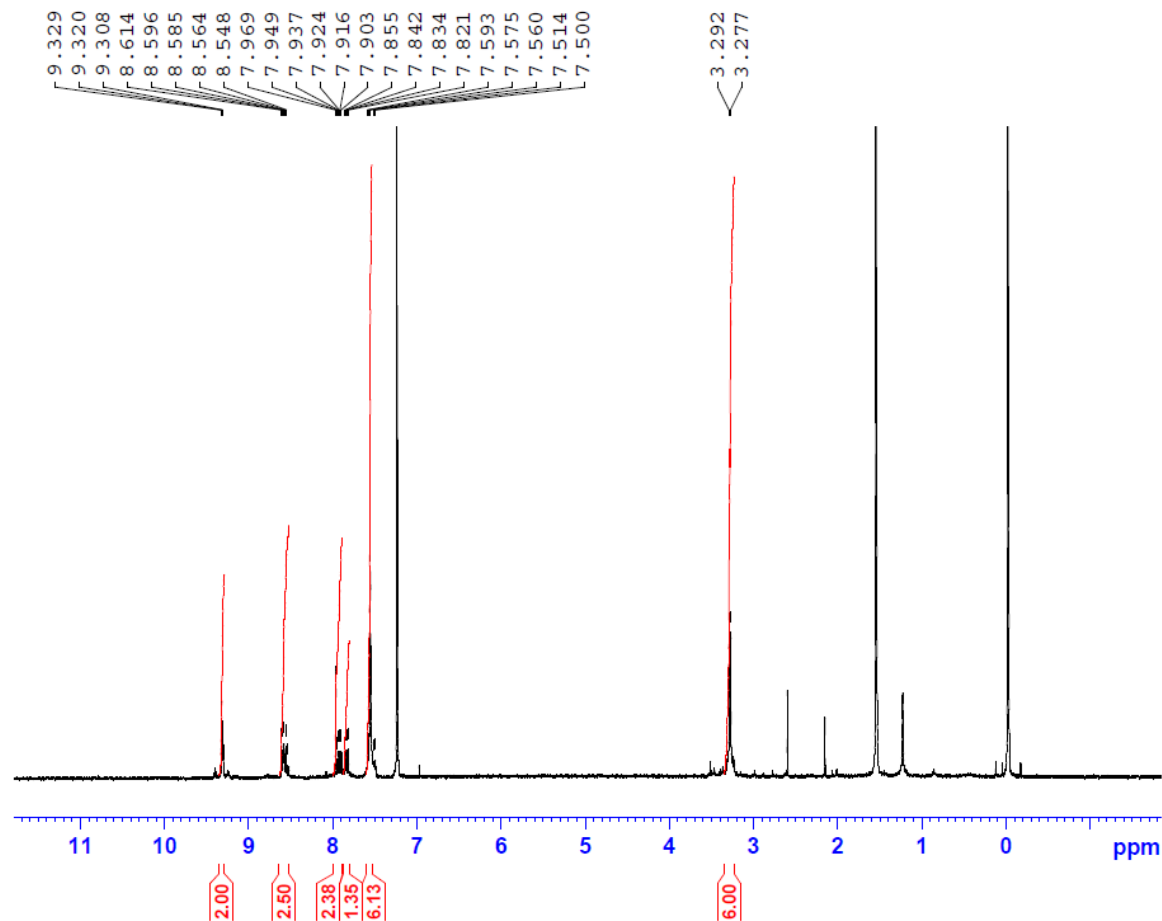


```
NAME          Fal Complex
EXPNO          36
PROCNO         1
Date_          20130131
Time           17.05
INSTRUM        spect
PROBHD         5 mm PABBO BB-
PULPROG        zg30
TD             65536
SOLVENT        CDCl3
NS             32
DS             2
SWH            8223.685 Hz
FIDRES         0.125483 Hz
AQ            3.9846387 sec
RG            203
DM            60.800 usec
DE            6.50 usec
TE            294.0 K
D1            1.00000000 sec
TDO           1
```

```
----- CHANNEL f1 -----
NUC1           1H
P1             14.04 usec
PL1            -2.00 dB
PL1W          17.39728355 W
SF01          400.1424710 MHz
SI            32768
SF            400.1400122 MHz
WDW            EM
SSB            0
LB             0.30 Hz
GB             0
PC             1.00
```

Fig S10. ^1H -NMR spectrum of $\text{Re}(\text{biq})(\text{CO})_3(\text{CN})\text{-}[\text{Pt}(\text{DMSO})(\text{Cl})_2]$ (1) (400 MHz, CDCl_3).

Re-001-CN-Pt-20130125



```
NAME          Fai complex
EXPNO          29
PROCNO         1
Date_          20130125
Time_          20.02
INSTRUM        spect
PROBHD         5 mm PABBO BB-
PULPROG        zg30
TD             65536
SOLVENT        CDCl3
NS             32
DS             2
SWH            8223.685 Hz
FIDRES         0.125483 Hz
AQ            3.9846387 sec
RG            203
DW            60.800 usec
DE            6.50 usec
TE            293.2 K
D1            1.00000000 sec
TD0           1
```

```
===== CHANNEL f1 =====
NUC1           1H
P1            14.04 usec
PL1           -2.00 dB
PL1W          17.39728355 W
SFO1          400.1424710 MHz
SI            32768
SF            400.1400122 MHz
WDW           EM
SSB           0
LB            0.30 Hz
GB            0
PC            1.00
```

Fig S11. ¹H-NMR spectrum of $\text{Re}(5\text{-ph-phen})(\text{CO})_3(\text{CN})\text{-}[\text{Pt}(\text{DMSO})(\text{Cl})_2]$ (2) (400 MHz, CDCl_3).

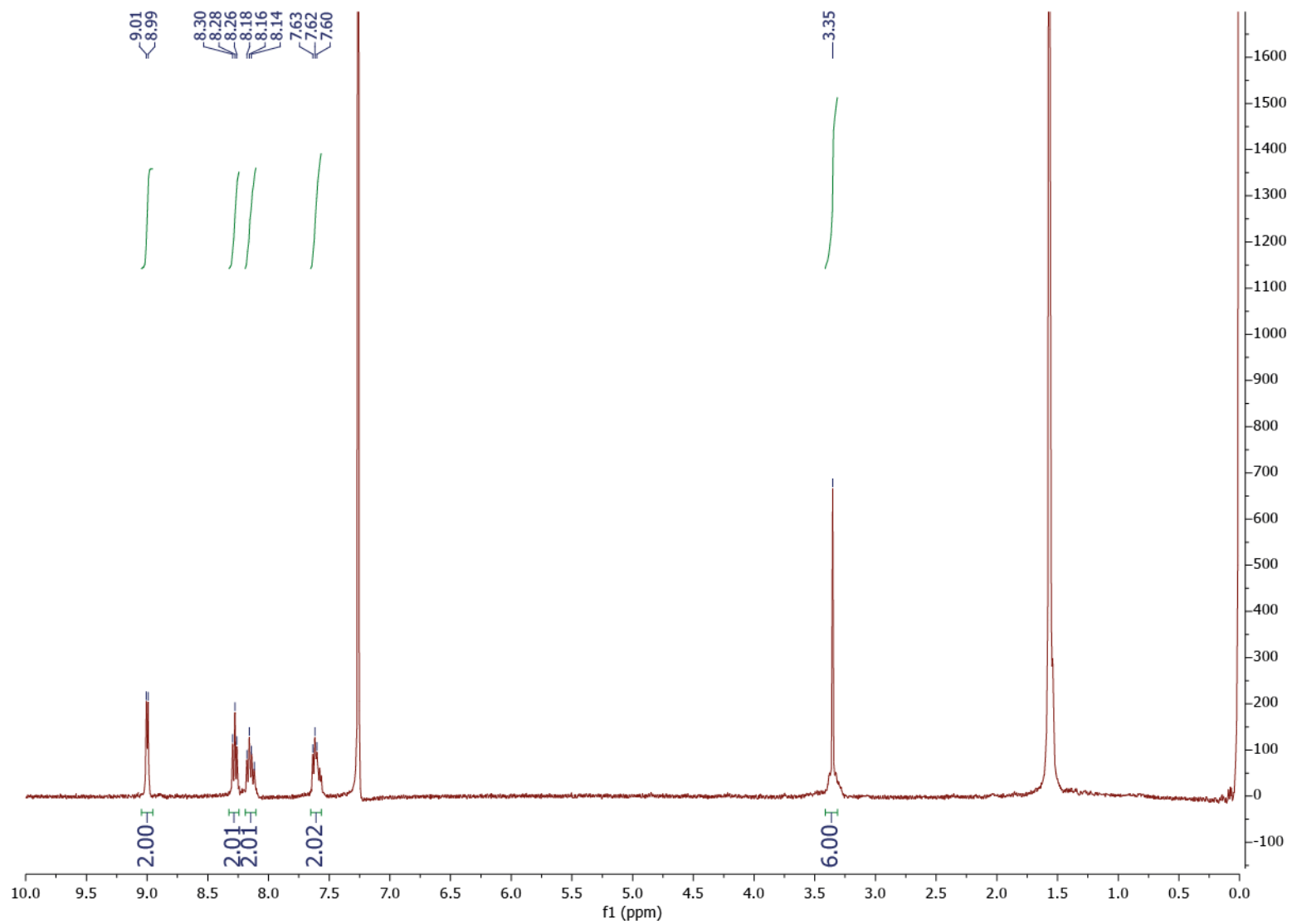


Fig S12. ¹H-NMR spectrum of $\text{Re}(\text{bpy})(\text{CO})_3(\text{CN})\text{-}[\text{Pt}(\text{DMSO})(\text{Cl})_2]$ (3) (400 MHz, CDCl_3).

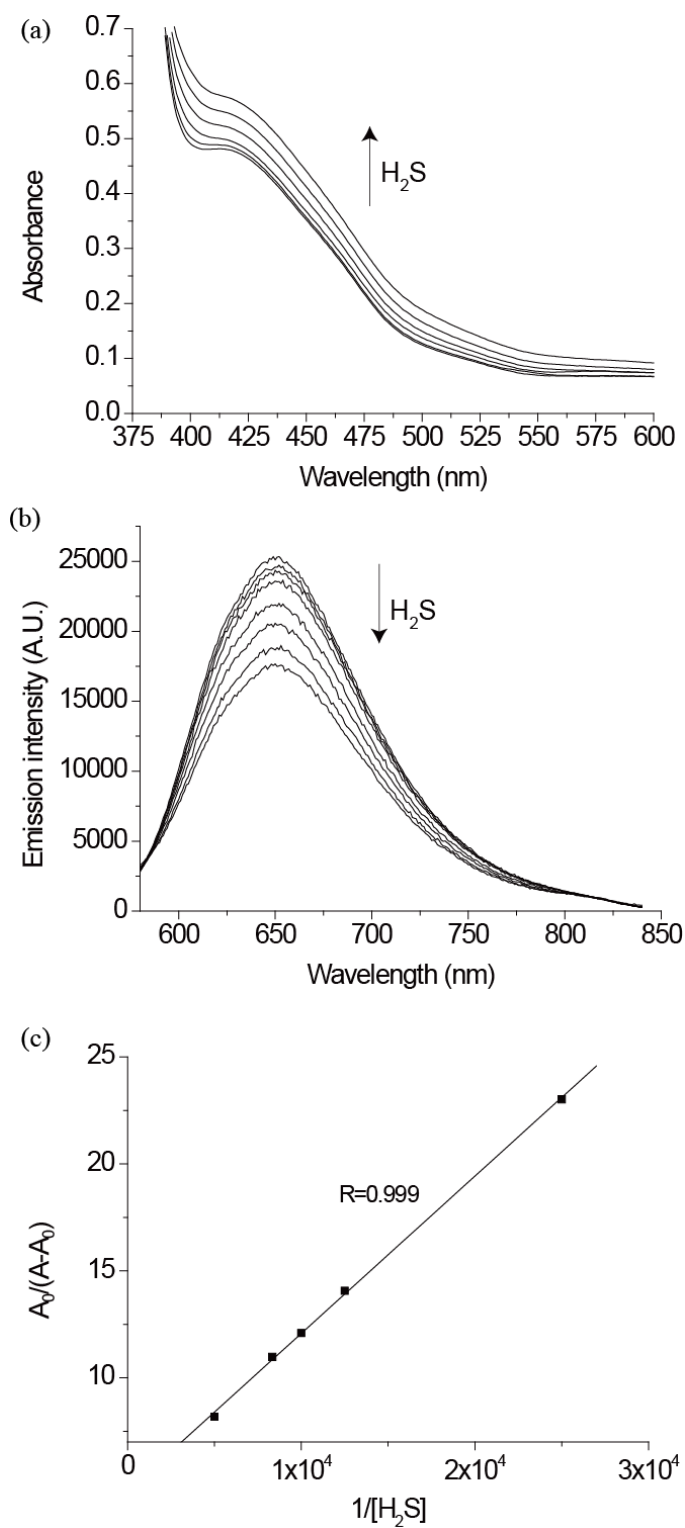


Fig S13. (a) UV-Vis absorption spectra and (b) spectrofluorimetric titrations of complex **1** (1×10^{-4} M) with H₂S (0 to 5×10^{-4} M) ($\lambda_{\text{ex}} = 432$ nm). (c) Plot of $A_0/(A-A_0)$ versus $1/[\text{H}_2\text{S}]$: Slope and y-intercept of the best-fit line are 7.36×10^{-4} M and 4.717, respectively, $\log K = 3.81 \pm 0.005$ at 330 nm. All titrations were carried out in CHCl₃ at 298 K.

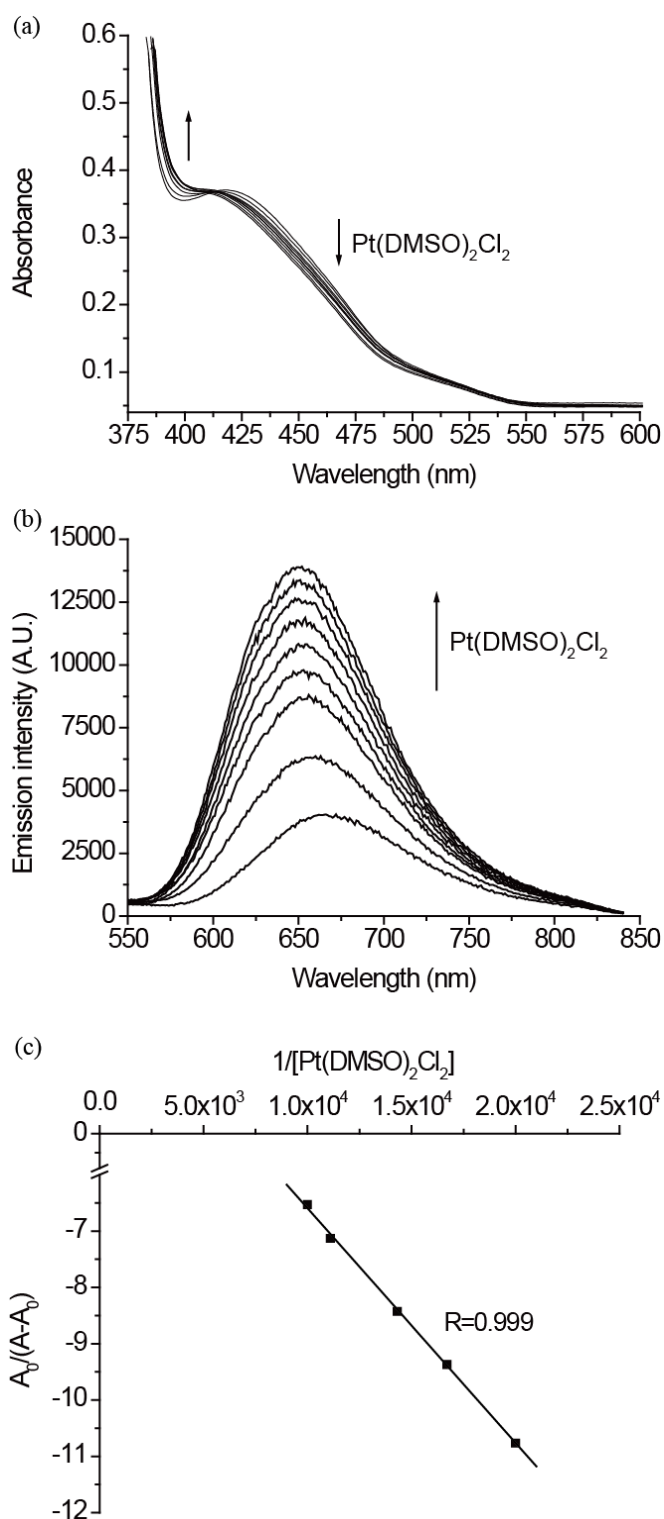


Fig S14. (a) UV-vis spectroscopic and (b) spectrofluorimetric titrations of $\text{Re}(\text{big})(\text{CO})_3(\text{CN})$ (1.0×10^{-4} M) with $\text{Pt}(\text{DMSO})_2\text{Cl}_2$ (0 to 1.0×10^{-4} M). (c) The slope and y-intercept are -4.17×10^{-4} M and -2.426 respectively of the best fitted $A_0/(A-A_0)$ versus $1/[\text{Pt}(\text{DMSO})_2\text{Cl}_2]$ plot with $\log K = 3.76 \pm 0.02$ at 450 nm. All titrations were carried out in MeOH/CHCl₃ mixture (v/v 1:1) at 298 K. Excitation $\lambda_{\text{ex}} = 432$ nm.

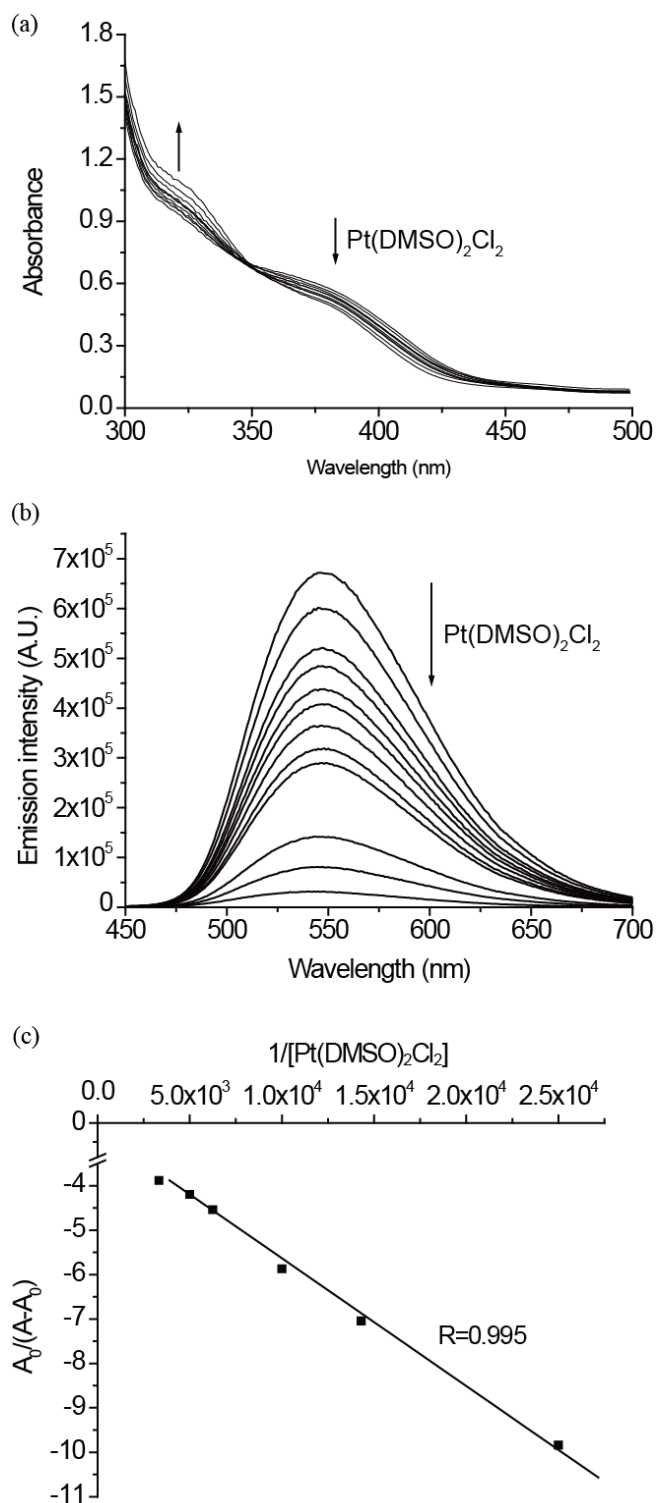


Fig S15. (a) UV-vis spectroscopic and (b) spectrofluorimetric titrations of $\text{Re}(5\text{-}ph\text{-}phen)(\text{CO})_3(\text{CN})$ (1.0×10^{-4} M) with $\text{Pt}(\text{DMSO})_2\text{Cl}_2$ (0 to 1.0×10^{-4} M). (c) The slope and y-intercept are -2.88×10^{-4} M and -2.757 respectively of the best fitted $A_0/(A-A_0)$ versus $1/[\text{Pt}(\text{DMSO})_2\text{Cl}_2]$ plot with $\log K = 3.98 \pm 0.04$ at 400 nm. All titrations were carried out in MeOH/ CHCl_3 mixture (v/v 1:1) at 298 K. Excitation $\lambda_{\text{ex}} = 363$ nm.

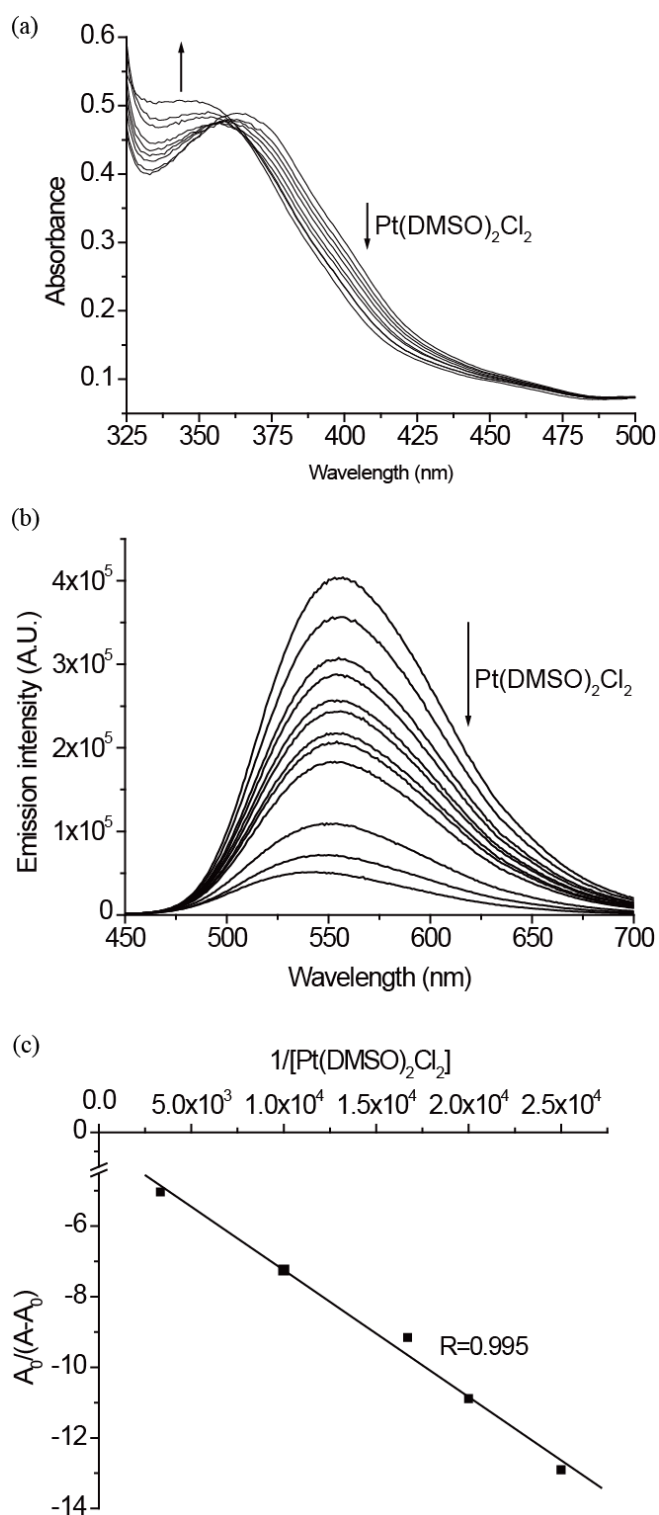


Fig S16. (a) UV-vis spectroscopic and (b) spectrofluorimetric titrations of $\text{Re}(\text{bpy})(\text{CO})_3(\text{CN})$ (1.0×10^{-4} M) with $\text{Pt}(\text{DMSO})_2\text{Cl}_2$ (0 to 1.0×10^{-4} M). (c) The slope and y-intercept are -3.59×10^{-4} M and -3.656 respectively of the best fitted $A_0/(A-A_0)$ versus $1/[\text{Pt}(\text{DMSO})_2\text{Cl}_2]$ plot with $\log K = 4.01 \pm 0.04$ at 400 nm. All titrations were carried out in MeOH/ CHCl_3 mixture (v/v 1:1) at 298 K. Excitation $\lambda_{\text{ex}} = 371$ nm.

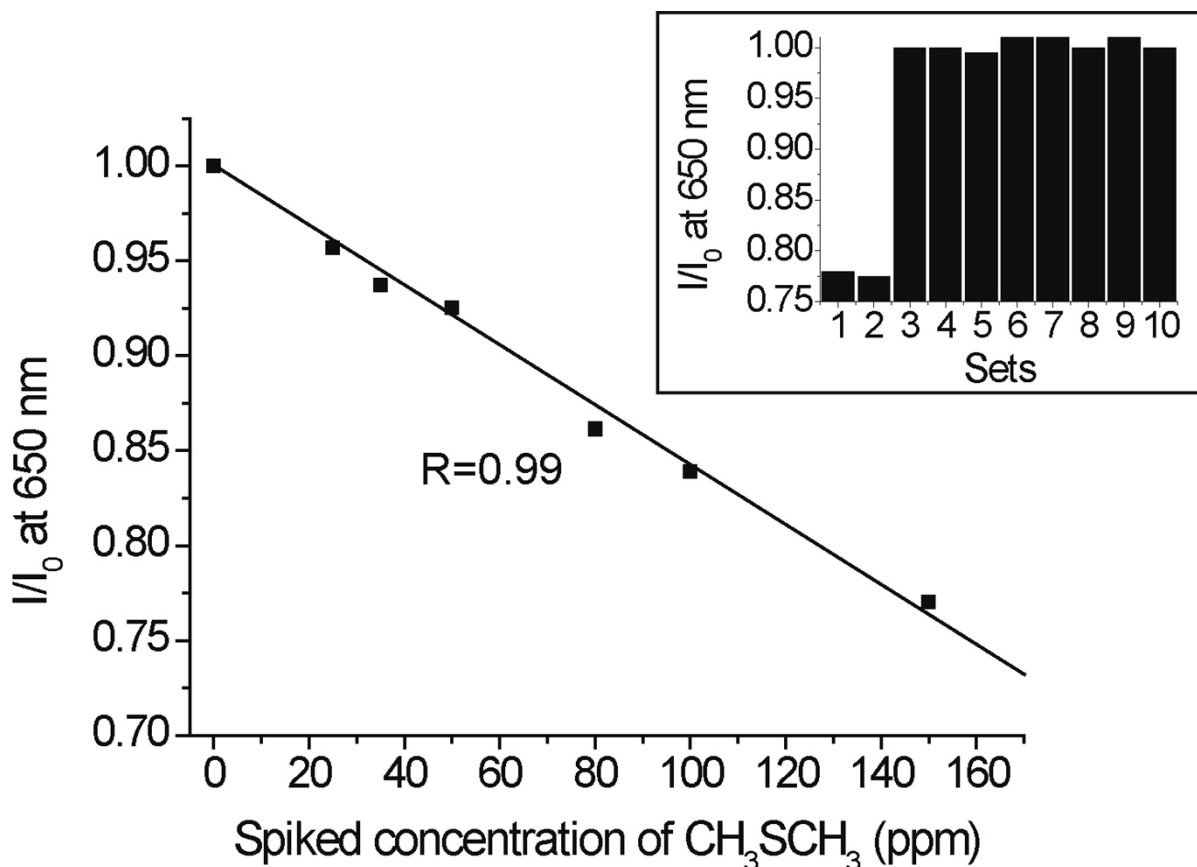


Fig 17. (Inset): Spectrofluorometric responses (I/I_0 at 650 nm) of complex **1** (1×10^{-4} M) toward a series of homogenized swine loin samples (20.0 g; *Sus scrofa domesticus*) stored in the presence of different vapors: (set 1) Dimethyl sulfide; (set 2) a mixture of dimethyl sulfide and common BVCs (dimethyl disulfide, dimethyl trisulfide, CO, triethylamine, propanoic acid, 4-ethylphenol, and CH₄; each at 150 ppm); (set 3–9) common BVCs (dimethyl disulfide, dimethyl trisulfide, CO, triethylamine, propanoic acid, 4-ethylphenol, and CH₄); and (set 10) a mixture of the common BVCs used in sets 3–9 (each at 150 ppm). Results of spectrofluorimetric titration of complex **1** (1×10^{-4} M) in the swine loin sample spiked with increasing concentration of CH₃SCH₃. The best-fit line of the plot of I/I_0 versus [CH₃SCH₃] revealed a slope and y-intercept of 1.59×10^{-3} and 1.00 ppm, respectively. All titrations were carried out in chloroform at 298 K.